arXiv:1412.0612v1 [hep-th] 1 Dec 2014

November 2014

Exoflops in Two Dimensions

Paul S. Aspinwall

Department of Mathematics
Duke University, Durham, NC 27708-0223

Abstract

An exoflop occurs in the gauged linear σ-model by varying the Kähler form so that a subspace appears to shrink to a point and then reemerge "outside" the original manifold. This occurs for K3 surfaces where a rational curve is "flopped" from inside to outside the K3 surface. We see that whether a rational curve contracts to an orbifold phase or an exoflop depends on whether this curve is a line or conic. We study how the D-brane category of the smooth K3 surface is described by the exoflop and, in particular, find the location of a massless D-brane in the exoflop limit. We relate exoflops to noncommutative resolutions.

1 Introduction

The venerable gauged linear σ-model [1] has been used in a wide variety of applications in the past 20 years. The key notion is that there is some Kähler moduli space that can be divided up into "phases" and these phases are asymptotically the cones in some secondary fan. Typical familiar and well-studied phases include large radius limits, orbifold and Landau–Ginzburg models. These are misleading, however, since they are not singular.[1] In a typical example with $h^{1,1} \gg 1$, one has a multitude of "exoflops" and "bad hybrids" [2,3] as singular phase limits. In this paper we study this somewhat neglected exoflop phase. In particular we will study them in the simplest setting they appear, namely dimension two.

An exoflop occurs when an algebraic subset is contracted by deforming the Kähler form. As one continues this deformation beyond the point of contraction, a new component of the gauged linear σ-model vacuum grows out external to the original space. The new component intersects the original space at a singularity resulting from the contraction. Only rational curves can be contracted in a K3 surface but we will see that their embedding in the ambient toric variety will determine whether an orbifold phase or an exoflop phase occurs on their contraction.

It is well-known that singular theories lurk in the walls dividing the phases from each other. It might appear, then, that there are two distinct sets of theories of particular interest:

- The phase limits that appear in the deep limit of each maximal cone in the secondary fan.
- The singular theories in the wall separating these limits.

There really is no such intrinsic dichotomy as has been noted before [4, 5]. In this paper we will compare how a singular theory can manifest itself dually as living in a wall or living in a limit in the simplest case. That is, we consider contracting a curve in a K3 surface such that the B-field is zero on this curve. In the past this has generally been considered as the singular theory that separates the large radius phase of the K3 surface from some orbifold phase. Here we will also manifest it as an exoflop limit in a gauged linear σ-model.

Naturally the intrinsic geometry, as viewed by a *non-linear* σ-model, of these two possibilities is identical and thus any associated physics in the string compactification would be identical. However, the presentation of the theories is quite different. In particular, the description of the D-branes will be not at all the same and we focus on this below.

The D-branes in an orbifold phase include fractional branes stuck at the orbifold point [6]. These "resolve" the category in the sense that they provide the objects in the derived category that appear when the orbifold point is blown up according to the McKay correspondence. In contrast to this we will see that these extra D-branes in an exoflop appear as matrix factorizations living at the North pole on the $\mathbb{P}^1$ sticking out of the singularity. This is more in the flavour of noncommutative resolutions as we discuss below.

[1] The large radius limit is, of course, singular at infinity but this is infinite distance in the moduli space and can be viewed in a controlled way as a decompactification. Our use of the term "singular" will mean at finite distance.

In section 2 we discuss the general difference between lines and conics as they are contracted in a K3 surface. We use the elegant technology of spherical functors to analyze the monodromy and thus D-brane behaviour. In section 3 we analyze two examples in detail to see how the D-branes understood geometrically in the smooth phase appear in the exoflop. In the second example we have a "double exoflop" where are chain of two $\mathbb{P}^1$'s are pushed out of the K3 surface.

2 Lines vs Conics

Consider a smooth curve C of degree m in $\mathbb{P}^2$. The case $m = 1$ is a line and the case $m = 2$ is a conic. They are both isomorphic to $\mathbb{P}^1$. We wish to extend this notion to more complicated embeddings $C \subset V$, where V can be, for example, a toric variety.

Definition 1 *Let $C \cong \mathbb{P}^1$ and consider an embedding $i : C \to V$, where V is a toric variety. Let m be the smallest positive integer such that there exists a line bundle $\mathscr{E}$ on V with $i^*\mathscr{E} = \mathscr{O}_C(m)$. If $m = 1$ we call C a line and if $m = 2$ we call C a conic.*

2.1 The Toric Construction

Let us quickly review the toric machinery we require. We refer to section 2 of [5] for details of the construction rather than copying it verbatim here. Here is a quick list of notation:

- N is a lattice of rank d with dual lattice M.
- $\mathscr{A}$ is a collection of n points lying in a hypersurface in N.
- Σ is a regular triangulation of $\mathscr{A}$ or, depending on context, a fan over that triangulation.
- $S = \mathbb{C}[x_1, \ldots, x_n]$ is the associated homogeneous coordinate ring and $B_\Sigma \subset S$ is the irrelevant ideal. S has an r-fold grading (the $\mathrm{U}(1)^r$-charges) , where $r = n - d$.
- $Z_\Sigma = (\mathbb{C}^n - V(B_\Sigma)/(\mathbb{C}^*)^r$ is the associated toric variety (or stack).
- W is the superpotential, an element of S invariant under $(\mathbb{C}^*)^r$.
- X_Σ is the critical point set (or stack) of W in Z_Σ.

The *secondary polytope* has vertices corresponding to regular triangulations of $\mathscr{A}$ [7]. There is a dual *secondary fan.* Let $\overline{\mathscr{M}}$ denote the corresponding toric variety. This is viewed as a natural compactification of the "moduli space of complexified Kähler forms" and is of dimension r.

Each regular triangulation of $\mathscr{A}$ corresponds to a phase and corresponds to a point in $\overline{\mathscr{M}}$. This point is called the "phase limit". The discriminant $\Delta \subset \overline{\mathscr{M}}$ is called the "principal

A-determinant" in [7]. Singular conformal field theories are contained in Δ and in the toric divisors in $\overline{\mathscr{M}}$.

A one-dimensional edge of the secondary polytope corresponds to a toric rational curve in $\overline{\mathscr{M}}$ "joining" two phase limits. This is associated to a perestroika (see section 7.2.C of [7]). This rational curve will intersect Δ at one point [5]. Thus, this rational curve has three interesting points — the two phase limits and the intersection with Δ.

2.2 Line Examples

The simplest construction to see a line C in a Calabi–Yau surface is non-compact (i.e., no superpotential). In this case $d = 2$, $\mathscr{A}$ is three collinear equally spaced points and $S = \mathbb{C}[x_0, x_1, x_2]$ with degrees $(-2, 1, 1)$.

There are two phases — either we use the middle point (associated to x_0) or we ignore it. If we use it then we have the large radius phase with Z the total space of $\mathscr{O}_C(-2)$. Here C is the rational curve $x_0 = 0$. The Picard group of Z is rank one and the line bundle $\mathscr{O}(1)$ on Z restricts to $\mathscr{O}_C(1)$ and thus we have a line.

The other phase is an orbifold with an A_1 singularity, i.e., $\mathbb{C}^2/\mathbb{Z}_2$. Going between the phases consists of blowing up the orbifold. Since the Picard group is rank one we may specify the complexified Kähler form as a complex number $B+iJ$. As is well-known [8,9], $B+iJ = \frac{1}{2}$ in this orbifold limit. The singular theory living between these phases has $B + iJ = 0$.

It is also not hard to give a compact K3 example. Let $n = 6$, $d = 4$ and the pointset $\mathscr{A}$ be given by coordinates

$$\begin{array}{c|cccc} x_0 & 1 & 0 & 0 & 0 \\ x_1 & 1 & 1 & 0 & 0 \\ x_2 & 1 & 0 & 1 & 0 \\ x_3 & 1 & 0 & 0 & 1 \\ x_4 & 1 & -6 & -4 & -1 \\ x_5 & 1 & -3 & -2 & 0 \end{array}$$

Then the bigrading of S (i.e., the matrix of charges) is

$$Q = \begin{pmatrix} -6 & 3 & 2 & 0 & 0 & 1 \\ 0 & 0 & 0 & 1 & 1 & -2 \end{pmatrix}, \tag{1}$$

with a superpotential $W = x_0 F(x_1, \ldots, x_5)$, where we can choose the Fermat

$$F = x_1^2 + x_2^3 + (x_3^{12} + x_4^{12})x_5^6. \tag{2}$$

There are four triangulations of the pointset $\mathscr{A}$ and thus four phases. These are analogous to the 4 phases of the octic threefold [10]. We have a large radius Calabi–Yau phase which is an elliptically-fibred K3 surface with a rational curve section C. Here C is given by $x_5 = 0$ and the line bundle $\mathscr{O}(0, 1)$ restricts to $\mathscr{O}_C(1)$ on C, which is therefore a line.

Another phase corresponds to an orbifold given as the sextic hypersurface in $\mathbb{P}^3_{\{6,4,1,1\}}$. Going from the above Calabi–Yau phase to this orbifold contracts C. Locally, near this orbifold resolution, this example is identical to the noncompact version of the line above.

2.2.1 Monodromy

In this section we review the following well-known fact:

Proposition 1 *The monodromy around the limit point corresponding to a contracted line in a K3 surface is that of a $\mathbb{Z}_2$-orbifold at otherwise large radius limit.*

First let us clarify what we mean by "otherwise large radius limit". In the compact case we assume that the Picard number of the K3 surface is at least 2. Let $J \in H^2(S, \mathbb{R}) \cap H^{1,1}(S)$ be the Kähler form. The limit in question is then such that $\langle \alpha, J \rangle \to \infty$ for any homology class α not proportional to the class of our contracted curve. The noncompact case is implicitly at this limit.

We can determine the behaviour of the phase limit induced by contracting a line C by way of the monodromy tricks that have been employed in various examples [11] using the elegant formulation of spherical functors [5, 12–14]. This language nicely avoids the messy procedure of having to compute periods in form of hypergeometric systems in more than one variable. We have a functor

$$\mathbf{F} : \mathbf{A} \to \mathbf{D}^{\mathrm{b}}(S), \tag{3}$$

from some triangulated category $\mathbf{A}$. If this satisfies certain conditions we may construct an automorphism $T_{\mathbf{F}}$ of $\mathbf{D}^{\mathrm{b}}(S)$. If $\mathbf{F}$ is injective on objects we will denote this as $T_{\mathbf{A}}$.

To simplify notation, let us assume the Picard number is exactly 2. Given that we have a contractible *line*, there must be two distinct primitive divisor classes, H and L, in the K3 surface S such that we have intersection numbers

$$H.C = 0, \qquad L.C = 1. \tag{4}$$

$C.C = -2$ implies that the divisor class of C is $hH - 2L$ for some integer h.

As in [5], we choose a 2-sphere in the moduli space of complexified Kähler forms. This 2-sphere is near the large radius limit for everything other than C. We have 3 interesting points on the sphere:

- 0: The large C limit.
- ∞: The limit point we go to upon contracting C.
- Δ: The point in the wall dividing the phases where we have a necessarily have a singular conformal field theory.

Let T_0, T_∞ and T_Δ denote the automorphisms of the derived category induced by monodromy around these points. The topology of a 2-sphere with 3 punctures implies $T_\infty = T_\Delta T_0$.

We may choose $T_0 = - \otimes \mathscr{O}(L)$.[2] We denote this autoequivalence as $\mathscr{O}(L)$ for brevity. Contracting C is an EZ-transformation of Horja [15], or more specifically a Seidel–Thomas twist [16]. In spherical functor language $T_\Delta = T_{\langle \mathscr{O}_C \rangle}$, where $\langle \mathscr{O}_C \rangle$ is the derived category of a point and the image of this point under the spherical functor $\mathbf{F}$ is $\mathscr{O}_C$. In terms of

[2] The ambiguity in this choice was discussed in [5].

physics, this signifies that a single stable D-brane, corresponding to $\mathscr{O}_C$, becomes massless at Δ [11, 17] thus inducing the singular theory.

If Φ is an autoequivalence of $\mathbf{D}^{\mathrm{b}}(S)$ then [5]

$$\Phi T_{\mathbf{F}} = T_{\Phi\mathbf{F}}\Phi. \tag{5}$$

We now compute

$$\begin{aligned} T_\infty^2 &= T_\Delta T_0 T_\Delta T_0 \\ &= T_{\langle\mathscr{O}_C\rangle}\mathscr{O}(L)T_{\langle\mathscr{O}_C\rangle}\mathscr{O}(L) \\ &= T_{\langle\mathscr{O}_C\rangle}T_{\langle\mathscr{O}_C(1)\rangle}\mathscr{O}(2L) \\ &= T_{\langle\mathscr{O}_C,\mathscr{O}_C(1)\rangle}\mathscr{O}(2L), \end{aligned} \tag{6}$$

where the last equality follows from a result due to Kuznetsov (see theorem 11 in [5]).

Now $\langle\mathscr{O}_C, \mathscr{O}_C(1)\rangle$ is the derived category of C and so $T_{\langle\mathscr{O}_C,\mathscr{O}_C(1)\rangle}$ is T_{i_*} where $i : C \to S$ is the inclusion map for a divisor. As in example 10 of [5], T_{i_*} is therefore tensoring by $\mathscr{O}(C)$. But $\mathscr{O}(C) = \mathscr{O}(hH - 2L)$ so we end up with

$$T_\infty^2 = \mathscr{O}(hH). \tag{7}$$

Now the monodromy $\mathscr{O}(hH)$ is what we would expect for a large radius limit. Note that H does not intersect C and so this is some "large radius" for "the rest" of the K3 surface away from the line C. The fact we need to go *twice* around ∞ corresponds to a quantum $\mathbb{Z}_2$-symmetry that we would expect from an orbifold. Thus we have proved the proposition.

In Kähler form language, the Poincaré dual of the complexified Kähler form can be written as

$$B + iJ = xH + yL, \tag{8}$$

were we go to the "otherwise large radius limit" by setting $x \to \infty$. As shown in [8], the point Δ corresponds to $y = 0$; and ∞ corresponds to $y = \frac{1}{2}$. That is, the B-field on C is zero for the singular conformal field theory and $\frac{1}{2}$ for the orbifold.

Note that the 2-sphere we chose in the moduli space with the points 0, ∞ and Δ needs to be deformed so that it generically lies in the interior of the moduli space as discussed in [5]. This process involves a choice that varies h and so h is not uniquely defined. Note also that in the noncompact example of the total space of $\mathscr{O}_C(-2)$ we effectively ignore H and get $T_\infty^2 = 1$.

2.3 A Conic Example

Let $n = 6$, $d = 4$ and the pointset $\mathscr{A}$ be given by

$$\begin{array}{c|cccc} x_0 & 1 & 0 & 0 & 0 \\ x_1 & 1 & -1 & 0 & 0 \\ x_2 & 1 & 1 & 0 & 0 \\ x_3 & 1 & 0 & 1 & 0 \\ x_4 & 1 & 0 & 0 & 1 \\ x_5 & 1 & -1 & -1 & -1 \end{array} .$$

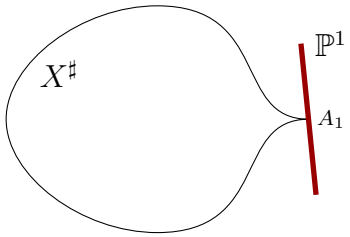

Figure 1: An exoflop.

Then the matrix of charges is

$$Q = \begin{pmatrix} -2 & -1 & 0 & 1 & 1 & 1 \\ -2 & 1 & 1 & 0 & 0 & 0 \end{pmatrix}, \tag{9}$$

with a superpotential $W = x_0 F(x_1, \ldots, x_5)$, where

$$F = x_1^2 f_4(x_3, x_4, x_5) + x_1 x_2 f_3(x_3, x_4, x_5) + x_2^2 f_2(x_3, x_4, x_5), \tag{10}$$

and f_k is a homogeneous equation of degree k. Let us assume that these f_k are generic to avoid unnecessary singularities.

There are four triangulations of the pointset $\mathscr{A}$ and thus four phases. Two of these phases are "hybrid" models which can be viewed as a fibration over a weighted projective space with fibre given by a Landau–Ginzburg theory. We will not be concerned with these hybrid phases in this paper.

Another phase is a large radius "Calabi–Yau" phase where $B = (x_1, x_2)(x_3, x_4, x_5)$. Here the ambient toric variety Z is a $\mathbb{P}^1$-bundle over $\mathbb{P}^2$. More precisely it is the bundle $\mathbb{P}(\mathscr{O} \oplus \mathscr{O}(-1))$ over $\mathbb{P}^2$. The constraints $\partial W/\partial x_i = 0$ force $x_0 = F = 0$. This yields that X is a double cover over $\mathbb{P}^2$ branched over the sextic $f_2 f_4 - f_3^2 = 0$. This is a smooth K3 surface and so we will call this the "smooth phase".

The other phase is the "exoflop" phase and has

$$B = (x_0, x_1) \cap (x_1, x_2) \cap (x_2, x_3, x_4, x_5). \tag{11}$$

The critical point set of W in this toric variety is reducible and has two components. One component has $x_0 = 0$. From (11) this forces $x_1 \neq 0$ and we may use one $\mathbb{C}^*$-action to set $x_1 = 1$. This leaves a quartic K3 surface in $\mathbb{P}^3$ with homogeneous coordinates $[x_2, x_3, x_4, x_5]$ given by

$$f_4(x_3, x_4, x_5) + x_2 f_3(x_3, x_4, x_5) + x_2^2 f_2(x_3, x_4, x_5) = 0. \tag{12}$$

This has an A_1 singularity at $[1, 0, 0, 0]$. The other component is a weighted projective space $\mathbb{P}^1_{\{2,1\}}$, which is isomorphic to $\mathbb{P}^1$, with homogeneous coordinates $[x_0, x_1]$ and with $[x_2, x_3, x_4, x_5] = [1, 0, 0, 0]$. The two components thus intersect at the A_1 point. The critical point set of W looks like figure 1, where $X^\sharp$ is the singular quartic K3.

One views the transition from the smooth phase to the exoflop phase as shrinking down the rational curve $C \subset X$ given by $x_1 = 0$. Then, after it has shrunk to point, one continues into the exoflop phase by "growing" the external $\mathbb{P}^1$ out of the resulting singularity.

The curve C is given by $f_2(x_3, x_4, x_5) = 0$ and is manifestly a conic in $\mathbb{P}^2$. Furthermore $\mathscr{O}(a, b)$ restricts to $\mathscr{O}_C(2a)$ so C is a conic by definition 1 too.

2.3.1 Monodromy

In this section we prove the following general result:

Proposition 2 *The monodromy around the limit point corresponding to a contracted conic in a K3 surface is the same as the monodromy around a singular conformal field theory equivalent to that of contracted line (with zero B-field) at otherwise large radius limit.*

Again we can use the language of spherical functors to calculate monodromies. Now we have divisor classes H and L such that

$$H.C = 0, \qquad L.C = 2. \tag{13}$$

Furthermore, $C.C = -2$ implies that the divisor class of C is $hH - L$ for some integer h.

Then

$$\begin{aligned} T_\infty &= T_\Delta T_0 \\ &= T_{\langle \mathscr{O}_C \rangle} \mathscr{O}(L) \\ &= T_{\langle \mathscr{O}_C \rangle} \mathscr{O}(C)^{-1} \mathscr{O}(hH) \\ &= T_{\langle \mathscr{O}_C \rangle} T^{-1}_{\langle \mathscr{O}_C(-1), \mathscr{O}_C \rangle} \mathscr{O}(hH) \\ &= T_{\langle \mathscr{O}_C \rangle} T^{-1}_{\langle \mathscr{O}_C \rangle} T^{-1}_{\langle \mathscr{O}_C(-1) \rangle} \mathscr{O}(hH) \\ &= T^{-1}_{\langle \mathscr{O}_C(-1) \rangle} \mathscr{O}(hH) \end{aligned} \tag{14}$$

Again, as in section 2.2.1 we have a large radius monodromy $\mathscr{O}(hH)$ coming from geometry away from the contraction. The more interesting part of the monodromy is the Seidel–Thomas [16] twist $T_{\langle \mathscr{O}_C(-1) \rangle}$, which is the monodromy associated to a single object $\mathscr{O}_C(-1)$ becoming massless. (Note the direction of the monodromy around ∞ is opposite to that around Δ and thus we have the inverse of a Seidel–Thomas twist for a massless D-brane.)

The nature of monodromy around ∞ is therefore identical (except for global geometric issues) the to monodromy around Δ. That is, we have a single massless D-brane, $\mathscr{O}_C$ at the discriminant Δ and another single massless D-brane $\mathscr{O}_C(-1)$ at the exoflop limit point ∞.

The B-field language is fairly clear. In the case of the line, $B = 0$ is at Δ and $B = \frac{1}{2}$ is at ∞. In the case of the conic we effectively double the B-field and so $B = 0$ at the Δ but now $B = 1$ at ∞. But $B = 1$ is the equivalent singular conformal field theory to $B = 0$ except that we need to relabel D-branes by a shift $- \otimes \mathscr{O}(-1)$. This is exactly what we see above. The location of the orbifold point at $B = \frac{1}{2}$ is not manifestly obvious in the exoflop picture.

3 Geometrical Picture of D-branes on an Exoflop

We see that the contracted conic curve produces a massless D-brane $\mathscr{O}_C(-1)$ in the exoflop limit. But denoting it $\mathscr{O}_C(-1)$ is using the language of the large radius smooth phase. What does this massless D-brane look like in terms of the exoflop phase? Rather than prove general statements, we will analyze the example of section 2.3 and then a more complicated example in section 3.6. We assume other cases will be similar.

3.1 The conic

First let us review the basic algebraic geometry of a conic. Consider $C \subset \mathbb{P}^2$ given by $f = z_0^2 - z_1 z_2 = 0$. A coherent sheaf $\tilde{M}$ on C is associated to an R-module, M, where

$$R = \frac{S}{(f)}, \quad S = \mathbb{C}[z_0, z_1, z_2]. \tag{15}$$

Clearly the module $R(n)$ yields $\mathscr{O}_C(2n)$. So which modules give $\mathscr{O}_C(\text{odd})$? The skyscraper sheaf of the point $[0, 0, 1]$ is given by the module $\text{coker}(z_0, z_1)$. This has an infinite free resolution

$$\cdots \xrightarrow{\left(\begin{smallmatrix} z_0 & z_1 \\ z_2 & z_0 \end{smallmatrix}\right)} R(-4)^{\oplus 2} \xrightarrow{\left(\begin{smallmatrix} z_0 & -z_1 \\ -z_2 & z_0 \end{smallmatrix}\right)} R(-3)^{\oplus 2} \xrightarrow{\left(\begin{smallmatrix} z_0 & z_1 \\ z_2 & z_0 \end{smallmatrix}\right)} \tag{16}$$

$$R(-2)^{\oplus 2} \xrightarrow{\left(\begin{smallmatrix} z_0 & -z_1 \\ -z_2 & z_0 \end{smallmatrix}\right)} R(-1)^{\oplus 2} \xrightarrow{(z_0 \ z_1)} R \longrightarrow M \longrightarrow 0.$$

But we also have

$$0 \longrightarrow \mathscr{O}_C(-1) \longrightarrow \mathscr{O}_C \longrightarrow \mathscr{O}_{\text{pt}} \longrightarrow 0, \tag{17}$$

and so (mixing sheaves and modules)

$$\cdots \longrightarrow R(-2)^{\oplus 2} \xrightarrow{\left(\begin{smallmatrix} z_0 & -z_1 \\ -z_2 & z_0 \end{smallmatrix}\right)} R(-1)^{\oplus 2} \longrightarrow \mathscr{O}_C(-1) \longrightarrow 0. \tag{18}$$

We may tensor this resolution by $R(n)$ to resolve $\mathscr{O}_C(2n-1)$. In the usual way [18] we associate infinite resolutions with matrix factorizations. This means that $\mathscr{O}_C(\text{odd})$ is associated to the graded matrix factorization

$$\begin{pmatrix} z_0 & z_1 \\ z_2 & z_0 \end{pmatrix} \begin{pmatrix} z_0 & -z_1 \\ -z_2 & z_0 \end{pmatrix} = f.\mathbf{1}, \tag{19}$$

of suitable degree.

3.2 Following $\mathscr{O}_C(-1)$

We can now use the above construction to build a matrix factorization for $\mathscr{O}_C(-1)$ in the K3 surface S. We can then use the well-known procedure of carrying this over to the exoflop phase and reinterpret it there. That is, we have an equivalence of D-brane categories from the smooth K3 phase to the exoflop phase:

$$\Phi : \mathbf{D}^{\mathrm{b}}(S) \to \mathbf{D}_{\mathrm{exo}}. \tag{20}$$

We would like to compute $\Phi(\mathscr{O}_C(-1))$.

The procedure of moving objects in the derived category between different phases has been discussed in [19–22]. Let $S = \mathbb{C}[x_0, x_1, \ldots]$ be the homogeneous coordinate ring of the toric variety Z. Assume we have a superpotential $W = x_0 F(x_1, x_2, \ldots)$ and let X be the Calabi–Yau manifold $x_0 = F = 0$.

Beginning in the Calabi–Yau phase we have a coherent sheaf which is described as an A-module M, where

$$A = \frac{\mathbb{C}[x_1, x_2, \ldots]}{(F)}. \tag{21}$$

This A-module can be associated with a graded matrix factorization. The procedure for doing this is a little tedious but is easily computed via computer algebra as explained in detail in [21]. Indeed, the procedure is built into Macaulay 2 as part of the mechanism for computing Ext groups [23]. The resulting matrix factorization consists of maps between free graded S-modules enhanced by an extra grading. This new degree is associated with R-symmetry of the underlying conformal field theory or is considered a "homological" grading. This process of producing a matrix factorization also reintroduces the variable x_0 (called X_1 in [23]). The triply-graded degrees of the variables are now

	R	Q_1	Q_2
x_0	2	-2	-2
x_1	0	-1	1
x_2	0	0	1
x_3	0	1	0
x_4	0	1	0
x_5	0	1	0

(22)

We can rephrase this data by taking the summand of the two free modules and writing a single matrix acting as an endomorphism on this larger free module. Thus we write a graded matrix factorization as

$$u : \bigoplus_{i=1}^{2s} S(\mathbf{q}_i) \to \bigoplus_{i=1}^{2s} S(\mathbf{q}_i). \tag{23}$$

The matrix representing u squares to W. The two original rank s S-modules may be reconstructed by taking even and odd homological degrees of the big module. Note that any finite complex of sheaves can similarly be converted into a finite matrix factorization.

The next ingredient is to find a tilting collection

$$T = \bigoplus_{i=1}^{r} S(\mathbf{t}_i), \tag{24}$$

where the degrees $\mathbf{t}_i$ fit inside an r-dimensional "window" to pass between the phases as described in [20]. Any matrix factorization of the form (23) is unchanged as it passes between the phases if all the degrees $\mathbf{q}_i$ are elements of $\{\mathbf{t}_1, \mathbf{t}_2, \ldots, \mathbf{t}_r\}$.

More generally we can manipulate the matrix factorization (23) to make an object whose degrees $\mathbf{q}_i$ fit inside the window. We can doing this by taking mapping cones to and from objects which are trivial thanks to the irrelevant ideal. This construction describes how to transport general objects between phases.

For definiteness let us use a specific smooth

$$F = x_1^2(x_3^4 + x_4^4 + x_5^4) + x_2^2(x_3x_4 - x_5^2). \tag{25}$$

for the example from section 2.3. We will prove the following key result

Proposition 3 *The matrix factorization obtained from $\mathscr{O}_C(-1)$ in the smooth phase passes unchanged into the exoflop phase. That is, the same matrix factorization that Macaulay 2 gives us can be used for this object in $\mathbf{D}_{\text{exo}}$.*

The tilting collection we want to use to be consistent with section 2.3.1 is given by[3]

$$\begin{array}{ccc} S(-2,-1) & S(-1,-1) & S(0,-1) \\ S(-2,-2) & S(-1,-2) & S(0,-2) \end{array} \tag{26}$$

Here we have the conic C given by $x_1 = 0$. Thus $\mathscr{O}_C$ is (the sheaf associated to the module given as) the cokernel of the map (x_1). The cokernel of $(x_1\ x_3\ x_5)$ gives the point $x_1 = x_3 = x_5$ on C. Therefore, as in section 3.1, the module associated to $\mathscr{O}_C(-1)$ is the kernel of the quotient map

$$k : \operatorname{coker}(x_1) \to \operatorname{coker}(x_1\ x_3\ x_5). \tag{27}$$

Feeding this module into Macaulay gives the matrix factorization:

```
{0, -1, 0}   | 0         0        -x_0x_1x_4^4-x_0x_1x_5^4 -x_0x_1x_3^3x_5
{0, -1, 0}   | 0         0        0                        -x_0x_1x_3^4-x_0x_1x_4^4-x_0x_1x_5^4
{-1, 0, -1}  | x_1       0        0                        0
{-1, 0, -1}  | 0         x_1      0                        0                                        ...
{-1, -2, 0}  | x_3       -x_5     0                        0
{-1, -2, -2} | -x_2^2x_5 x_2^2x_4 0                        0
{-2, -1, -1} | 0         0        -x_3                     x_5
{-2, -1, -3} | 0         0        x_2^2x_5                 -x_2^2x_4
      ^^^^^^
      q_i
```

[3]By consistent we mean that the monodromy T_Δ is correctly determined by the tilting collection. The process of deriving T_Δ from a tilting collection was described in [20] (see also [24]). One essentially computes $T_\Delta = T_0^{-1}T_\infty$ where both T_0 and T_∞ are given by the same degree shift. For this case we use a degree shift of $(1, -1)$.

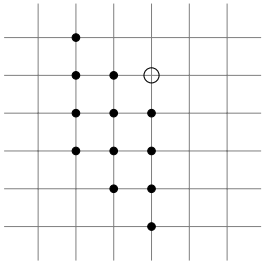

Figure 2: Extended window for the exoflop transition.

We do not care about the contents of this matrix, only the degrees. The degrees $\mathbf{q}_i$ are read off as the second and third entries as shown above (the first being the homological degree). Clearly they do not all lie in the tilting collection so we need to manipulate this object to fit it into the window.

The irrelevant ideal of both the Calabi–Yau phase and the exoflop phase is contained in the ideal (x_1, x_2). It follows that the complex

$$0 \longrightarrow S(1,-2) \xrightarrow{\binom{-x_2}{x_1}} \begin{matrix} S(1,-1) \\ \oplus \\ S(0,-1) \end{matrix} \xrightarrow{(x_1\ x_2)} S \longrightarrow 0, \tag{28}$$

is annihilated by the irrelevant ideal in both phases and is therefore trivial in the D-brane category in both phases. We now use this complex, and its degree shifts, to extend our window. That is, if three of the four $S(\mathbf{q}_i)$'s in (28) (or its shifts) appear in our tilting collection then we will add the fourth one. Then iterate this process.

This procedure leads to a collection of $\mathbf{q}_i$'s as shown in figure 2, where the circle represents the origin.

Now all the degrees appearing in the matrix factorization for $\mathscr{O}_C(-1)$ appear in this collection. This means we can build the matrix factorization out of objects in the tilting collection and objects which are trivial in both phases. This means we can copy this matrix factorization unchanged from the smooth phase into the exoflop phase and we prove the proposition.

3.3 Locating $\mathscr{O}_C(-1)$

Since the matrix factorization for $\mathscr{O}_C(-1)$ passed unchanged to the exoflop phase we can retain its interpretation as the kernel of the map (27). This allows us to locate it precisely. In particular it is supported at $x_1 = 0$. The irrelevant ideal (11) forces $x_0 \neq 0$. Since the K3 surface component of the exoflop has $x_0 = 0$ we see that this D-brane is not located there.

The other component of the exoflop, the $\mathbb{P}^1$ sticking out, has homogeneous coordinates $[x_0, x_1]$ and thus the D-brane $\mathscr{O}_C(-1)$ is located on here at the "other end" of the $\mathbb{P}^1$ from where it attached to the K3 component. We depict this in figure 3. From now on we will

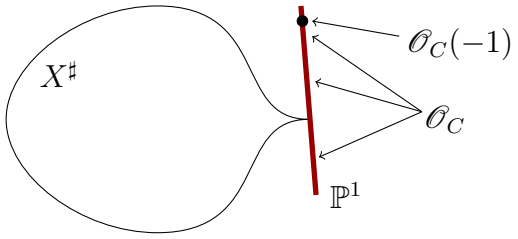

Figure 3: $\mathscr{O}_C(-1)$ located.

use "North pole" to denote the location of $\mathscr{O}(-1)$ on $\mathbb{P}^1$ and "South pole" to denote the intersection with $X^\sharp$.

Another case of interest corresponds to the cokernel of $(x_0\, x_1)$. This module corresponds to $\mathscr{O}_C$ in the smooth phase. A resolution of this module does not fit in the window or even the extended window of figure 2. We are forced to "prepare it" by applying a mapping cone with coker$(x_3\, x_4\, x_5)$ to get it into the window. Now when we pass into the exoflop phase, the object coker$(x_3\, x_4\, x_5)$ is supported all along the external $\mathbb{P}^1$. Thus, $\mathscr{O}_C$ is not supported just at the North pole — it is spread over the whole $\mathbb{P}^1$ as depicted in figure 2.

It is worth pointing out that no object can be localized at a single point on the external $\mathbb{P}^1$ other than the poles. The homogeneous coordinates are $[x_0, x_1]$. It follows that any such object would be associated with a module as the cokernel of a matrix involving $ax_0 + bx_1$, where a and b are nonzero and might involve other coordinates. Such any expression can never be homogeneous with respect to the grading (22). We therefore see that the exoflop is unphysical in the sense that no point-like D-brane can "move" along the external $\mathbb{P}^1$.

3.4 The gauged linear σ-model paradigm

We have argued that, in the case of contracting a conic, the singular conformal field theory appearing in the wall between the phases is essentially identical to that of the phase limit. Both theories involve a single D-brane becoming massless. Singularities appear in the gauged linear σ-model because the space on which the theory is defined becomes noncompact.

The potential for bosonic fields is [1, 25]

$$U = \sum_a \frac{D_a}{2e^2} + 2\sum_{a,b} \bar{\sigma}_a \sigma_b \sum_i Q_i^a Q_i^b |x_i|^2 + \sum_i \left| \frac{\partial W}{\partial x_i} \right|^2 . \tag{29}$$

There are two standard ways the vacuum for $U = 0$ can become noncompact and then we also have the exoflop way as we explain below.

The first type of singularity is the prototypical way we expect singularities to appear in the Kähler moduli space. As we move in the moduli space of complexified Kähler forms we vary parameters in D_a. Setting $D_a = 0$ then fixes values for $|x_i|^2$. At the walls in the phase picture we have $|x_i|^2 = 0$ and thus some of the σ fields become unconstrained and

noncompact. This is why we have singularities along the discriminant Δ as explained in detail in [25].

The second type of singularity is the prototypical way we expect singularities to appear in the complex structure moduli space. In this case we decompactify the vacuum by deforming the complex structure to acquire a singularity. If $W = x_0 F(x_1, x_2, \ldots)$ then

$$\sum_{i=0} \left| \frac{\partial W}{\partial x_i} \right|^2 = |F|^2 + |x_0|^2 \sum_{i=1} \left| \frac{\partial F}{\partial x_i} \right|^2 . \tag{30}$$

Thus, at a singularity where $F = \partial F/\partial x_i = 0$ the field associated to x_0 can go off to infinity.

The singularity at the exoflop limit is essentially equivalent to this latter complex-structure-induced singularity but it is obtained by varying the Kähler form. In the exoflop phase, the $X^\sharp$ component is singular, i.e., it has a solution of $F = \partial F/\partial x_i = 0$. Thus x_0 is liberated here which is why we have another $\mathbb{P}^1$ component attached at this point. But this $\mathbb{P}^1$ is *compact* and so the theory is not singular until we go all the way to the exoflop limit. In this limit the area of the external $\mathbb{P}^1$ is infinite (in the gauged linear σ-model picture) and so the vacuum is not compact.

3.5 The noncommutative resolution paradigm

The noncommutative resolution of [26] is a purely algebraic way of resolving a singularity. The idea is as follows (see also [27]). Suppose the singular variety is affine $X = \operatorname{Spec} R$. Then the fact that X is singular is reflected in the fact that R has infinite global dimension. That is, there is an R-module M that does not have a finite free resolution. We then use M to "blow-up" X.

For simplicity assume X is a hypersurface singularity. (Indeed these are the only examples studied to date.) Then the infinite free resolution of M corresponds to a matrix factorization. We can then define and analyze the algebra

$$A = \operatorname{End}(R \oplus M). \tag{31}$$

If this algebra has finite global dimension we are done. If not, we repeat the process and add in more modules.

When the process is complete we expect an equivalence of categories

$$\mathbf{D}^{\mathrm{b}}(\tilde{X}) \simeq \mathbf{D}^{\mathrm{b}}(\text{mod-}A), \tag{32}$$

where $\tilde{X}$ is a crepant resolution of X. Note that $R \oplus M$ is acting like a tilting object in this case, and that tilting objects cannot exist on a compact Calabi–Yau because of Serre duality. Thus noncommutative resolutions would seem necessarily restricted to describing noncompact geometries.

In the case of an A_1 singularity $z_0^2 - z_1 z_2 = 0$ in $\mathbb{C}^3$ the required matrix factorization for M is (19).

We claim the exoflop gives a very satisfying geometric description of the this non-geometric construction and indicates how to fit noncommutative resolutions into compact Calabi–Yau's. In our K3 case the matrix factorization that "smooths" the singularity in $X^\sharp$ is precisely the D-brane living at the North pole of the $\mathbb{P}^1$.

3.6 Exoflop Chains

We consider another example to get a better idea of the generic appearance of exoflops in K3 surfaces. Let $n = 7$, $d = 4$ and the pointset $\mathscr{A}$ be given by coordinates

$$\begin{array}{c|cccc} x_0 & 1 & 0 & 0 & 0 \\ x_1 & 1 & -2 & -1 & 0 \\ x_2 & 1 & -1 & -1 & -1 \\ x_3 & 1 & -1 & 0 & 1 \\ x_4 & 1 & 0 & 0 & 1 \\ x_5 & 1 & 0 & 1 & 0 \\ x_6 & 1 & 1 & 0 & 0 \end{array}$$

Then the trigrading of S is

$$Q = \begin{pmatrix} -2 & 0 & 0 & 1 & 0 & 0 & 1 \\ 0 & 1 & 0 & -2 & 0 & 1 & 0 \\ -2 & -1 & 1 & 1 & 1 & 0 & 0 \end{pmatrix}, \tag{33}$$

with a superpotential $W = x_0 F(x_1, \ldots, x_5)$. If we consider only the monomials at the vertices of the Newton polytope this polynomial would be

$$F = x_1^4 x_2^4 x_3^2 + x_1^4 x_3^2 x_4^4 + x_3^2 x_5^4 + x_2^2 x_6^2 + x_4^2 x_6^2. \tag{34}$$

The Kähler moduli space has dimension $r = 3$. The pointset has 12 triangulations. One of these phases yields X_Σ as a K3 surface given as a double cover of a Hirzebruch surface $\mathbb{F}_1$ branched over a suitable curve.

The 3-dimensional secondary polytope in this case is shown in figure 4. It is interesting to focus on one of the pentagonal faces of this polytope as shown in figure 5. These phases are as follows

1: $B = (x_1, x_5) \cap (x_1, x_6) \cap (x_3, x_6) \cap (x_2, x_3, x_4) \cap (x_2, x_4, x_5)$. This phase is a smooth K3 (a flop of the double cover of $\mathbb{F}_1$).

2: $B = (x_3) \cap (x_1, x_6) \cap (x_2, x_4, x_5)$. A singular K3 with two distinct A_1 singularities.

3: $B = (x_0, x_1) \cap (x_1, x_5) \cap (x_1, x_6) \cap (x_3, x_6) \cap (x_2, x_4, x_5)$. An exoflop. One component is a K3 surface which is a double cover branched over a nodal sextic. This surface has an A_1 singularity. The other component is isomorphic to $\mathbb{P}^1$ with coordinates $[x_0, x_1]$.

4: $B = (x_3) \cap (x_0, x_1) \cap (x_1, x_6) \cap (x_2, x_4, x_5, x_6)$. An exoflop. One component is a quartic K3 surface with an A_3 singularity. The other component is a $\mathbb{P}^1$ with homogeneous coordinates $[x_0, x_1]$.

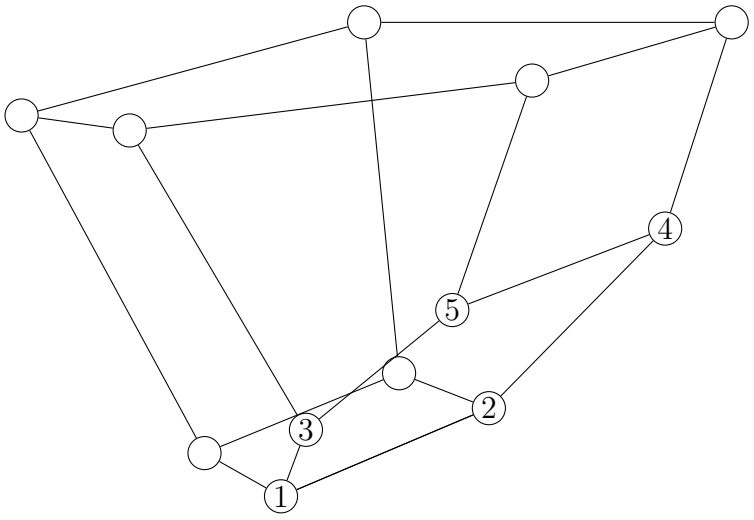

Figure 4: The secondary polytope for section 3.6.

5: $B = (x_0, x_1) \cap (x_0, x_3) \cap (x_1, x_5) \cap (x_1, x_6) \cap (x_3, x_6) \cap (x_2, x_4, x_5, x_6)$. A "double exoflop". One component is a quartic K3 surface with an A_3 singularity. There are two other components each isomorphic to $\mathbb{P}^1$ forming a chain off this singular point. These $\mathbb{P}^1$'s have coordinates $[x_0, x_3]$ and $[x_1, x_5]$.

It is very interesting following the D-branes between these phases. In phase 1 everything is smooth. This K3 surface contains a chain of 3 rational curves. The central curve is a conic and the two outside are lines. Moving to phase 2 we contract the two lines to orbifold singularities and moving to phase 3 we contract the conic to an exoflop phase all as expected from section 2. In phase 3 we have one matrix factorization living at the North pole as shown in the figure.

An interesting thing happens when we move from phase 1 to phase 3. We bring the two lines together and they become a (singular) conic. Accordingly, when we move to phase 5 these conics must induce another exoflop. This pushes out the already exoflopped $\mathbb{P}^1$ producing a chain of two external $\mathbb{P}^1$'s.

On the other side of the pentagon in figure 5 we can contract the conic in phase 2 to produce an exoflop, phase 4. This pushes 3 matrix factorizations onto the North pole. In this sense, phase 4 represents the noncommutative resolution of the A_3 singularity. If we represent an A_3 singularity as $z_0^4 - z_1 z_2$ then the noncommutative resolution using the

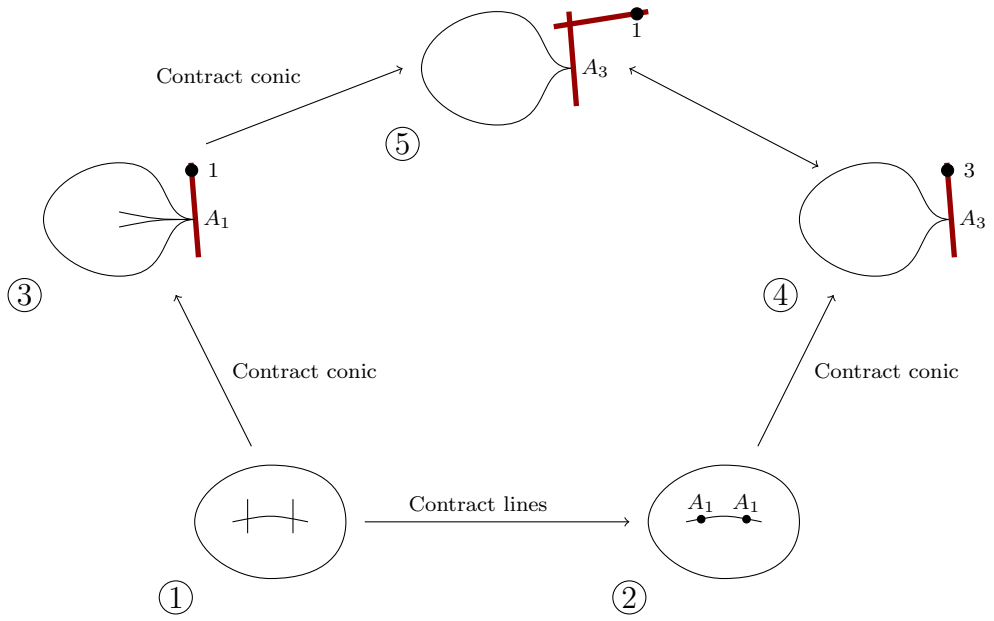

Figure 5: A face of the secondary polytope.

methods in [27] is given by the quiver

$$\begin{array}{ccc} R & \underset{(z_2\ -z_0)}{\overset{\binom{0}{1}}{\rightleftarrows}} & \operatorname{coker}\begin{pmatrix} z_1 & z_0 \\ z_0^3 & z_2 \end{pmatrix} \\ {\scriptstyle (-z_0\ z_1)}\uparrow\downarrow{\scriptstyle \binom{1}{0}} & & {\scriptstyle \binom{1\ 0}{0\ z_0}}\uparrow\downarrow{\scriptstyle \binom{z_0\ 0}{0\ 1}} \\ \operatorname{coker}\begin{pmatrix} z_1 & z_0^3 \\ z_0 & z_2 \end{pmatrix} & \underset{\binom{z_0\ 0}{0\ 1}}{\overset{\binom{1\ 0}{0\ z_0}}{\rightleftarrows}} & \operatorname{coker}\begin{pmatrix} z_1 & z_0^2 \\ z_0^2 & z_2 \end{pmatrix} \end{array} \tag{35}$$

The 3 matrix factorizations at the North pole in phase 4 correspond to the 3 matrix factorizations in this quiver.

Passing from phase 4 to phase 5 is a new transition that we haven't explored. The 3 matrix factorizations on the North pole in phase 4 are "blown-up" to produce the extra $\mathbb{P}^1$ in the double exoflop.

Let us note that the exoflop behaviour here occurs because the A_3 singularity manifests itself as a hypersurface singularity of the form $z_0^4 - z_1 z_2$. If the singularity had appeared instead because of an orbifold singularity in the ambient toric variety then we would have expected orbifold phases rather than exoflop .

Generalizing this example we would expect an A_{2k-1} singularity in a K3 surface that presented itself as a hypersurface singularity $z_0^{2k} - z_1 z_2$ to have a phase where a chain of k $\mathbb{P}^1$'s protrudes out from the singularity.

4 Discussion

A typical hypersurface (or complete intersection) Calabi–Yau in a toric variety has a huge number of phases and many of these phases involve exoflops. This is true even for K3 surfaces as we have explored in this paper. The exoflop seems to give a useful presentation of the derived category (i.e., D-brane category) by manifestly "splitting off" some objects by sending them to the North pole of an exoflopped $\mathbb{P}^1$. While a semiorthogonal decomposition for a compact Calabi–Yau is impossible because of Serre duality, exoflops perhaps provide a useful alternative in some sense.

We might regard something akin to phase 4 in figure 5 where the matrix factorizations associated to the noncommutative resolution all live at the North pole of a single $\mathbb{P}^1$ to be the most useful picture, or it may be that the exoflop chain in phase 5 proves the best "decomposition" of the D-brane category. In particular, it would be interesting, therefore, to have a general understanding of the transitions of the type between phases 4 and 5.

The structure of exoflops is much richer for Calabi–Yau threefolds than for the case of dimension two we considered in this paper. More importantly, exoflops are intimately connected to extremal transitions in this case. The transitions that connect the web of Calabi–Yau hypersurfaces in toric varieties as studied in [28] all go via exoflop limits. A flavour of this is seen in the K3 surface as such transitions connect algebraic families of of K3's of different generic Picard number. The example in section 2.3 has generic Picard number 2 but in the exoflop phase we have a quartic K3 surface. The analogue of an extremal transition would be to ignore the exoflopped $\mathbb{P}^1$ and deform the complex structure of the remaining part to a generic quartic with Picard number one.

This explicit exoflop picture of an extremal transition must surely shed some light on the way the derived category changes as one passes between topologically distinct Calabi–Yau threefolds.

Another kind of phase is intimately connected to the exoflop phase. This is the "bad hybrid" model of [2, 3]. We can get a bad hybrid model from figure 1 by collapsing $X^\sharp$ to a point using a Calabi–Yau to Landau–Ginzburg transition. All that remains is a $\mathbb{P}^1$ but it has two special points. At the North pole there is $\mathscr{O}_C(-1)$ and at the South pole there are many matrix factorizations that account for many the D-branes in $X^\sharp$. As in the exoflop case, the grading prohibits the existence of any D-brane localized at a point on the $\mathbb{P}^1$ except at the poles.

In a typical example with many phases, most phases would appear to involve exoflops or bad hybrids. Given the equivalence of the D-brane category between all the phases, it seems certain that these phases are worthy of more attention.

Acknowledgments

I thank N. Addington and R. Plesser for many useful and important discussions. This work was partially supported by NSF grant DMS–1207708. Any opinions, findings, and conclusions or recommendations expressed in this material are those of the author and do

not necessarily reflect the views of the National Science Foundation.

References

[1] E. Witten, *Phases of $N = 2$ Theories in Two Dimensions*, Nucl. Phys. **B403** (1993) 159–222, hep-th/9301042.

[2] P. S. Aspinwall and M. R. Plesser, *Decompactifications and Massless D-Branes in Hybrid Models*, JHEP **1007** (2010) 078, arXiv:0909.0252.

[3] M. Bertolini, I. V. Melnikov, and M. R. Plesser, *Hybrid Conformal Field Theories*, JHEP **1405** (2014) 043, arXiv:1307.7063.

[4] B. R. Greene, D. R. Morrison, and C. Vafa, *A Geometric Realization of Confinement*, Nucl. Phys. **B481** (1996) 513–538, hep-th/9608039.

[5] N. Addington and P. S. Aspinwall, *Categories of Massless D-Branes and del Pezzo Surfaces*, JHEP **1307** (2013) 176, arXiv:1305.5767.

[6] M. R. Douglas and G. Moore, *D-branes, Quivers, and ALE Instantons*, hep-th/9603167.

[7] I. M. Gelfand, M. M. Kapranov, and A. V. Zelevinski, *Discriminants, Resultants and Multidimensional Determinants*, Birkhäuser, 1994.

[8] P. S. Aspinwall, B. R. Greene, and D. R. Morrison, *Measuring Small Distances in $N = 2$ Sigma Models*, Nucl. Phys. **B420** (1994) 184–242, hep-th/9311042.

[9] P. S. Aspinwall, *Enhanced Gauge Symmetries and K3 Surfaces*, Phys. Lett. **B357** (1995) 329–334, hep-th/9507012.

[10] P. Candelas et al., *Mirror Symmetry for Two Parameter Models — I*, Nucl. Phys. **B416** (1994) 481–562, hep-th/9308083.

[11] P. S. Aspinwall, *D-Branes on Calabi–Yau Manifolds*, in J. M. Maldacena, editor, "Progress in String Theory. TASI 2003 Lecture Notes", pages 1–152, World Scientific, 2005, hep-th/0403166.

[12] R. Rouquier, *Categorification of $\mathfrak{sl}_2$ and braid groups*, in "Trends in representation theory of algebras and related topics", Contemp. Math. **406**, pages 137–167, Amer. Math. Soc., Providence, RI, 2006.

[13] R. Anno, *Spherical Functors*, arXiv:0711.4409.

[14] N. Addington, *New derived symmetries of some hyperkähler varieties*, arXiv:1112.0487.

[15] R. P. Horja, *Derived Category Automorphisms from Mirror Symmetry*, math.AG/-0103231.

[16] P. Seidel and R. P. Thomas, *Braid Groups Actions on Derived Categories of Coherent Sheaves*, Duke Math. J. **108** (2001) 37–108, math.AG/0001043.

[17] P. S. Aspinwall and M. R. Douglas, *D-Brane Stability and Monodromy*, JHEP **05** (2002) 031, hep-th/0110071.

[18] D. Eisenbud, *Homological Algebra on a Complete Intersection, with an Application to Group Representations*, Trans. Amer. Math. Soc. **260** (1980) 35–64.

[19] D. Orlov, *Derived Categories of Coherent Sheaves and Triangulated Categories of Singularities*, in "Algebra, Arithmetic, and Geometry: in Honor of Yu. I. Manin. Vol. II", Progr. Math. **270**, pages 503–531, Birkhäuser Boston Inc., Boston, MA, 2009, math.AG/0503632.

[20] M. Herbst, K. Hori, and D. Page, *Phases Of $N = 2$ Theories In $1 + 1$ Dimensions With Boundary*, arXiv:0803.2045.

[21] P. S. Aspinwall, *Topological D-Branes and Commutative Algebra*, hep-th/0703279, submitted to Communications in Number Theory and Physics.

[22] E. Segal, *Equivalence Between GIT Quotients of Landau-Ginzburg B-models*, Comm. Math. Phys. **304** (2011) 411–432.

[23] L. L. Avramov and D. R. Grayson, *Resulutions and Cohomology over Complete Intersections*, in D. Eisenbud et al., editors, "Computations in Algebraic Geometry with Macaulay 2", Algorithms and Computations in Mathematics **8**, pages 131–178, Springer-Verlag, 2001.

[24] D. Halpern-Leistner and I. Shipman, *Autoequivalences of derived categories via geometric invariant theory*, arXiv:1303.5531.

[25] D. R. Morrison and M. R. Plesser, *Summing the Instantons: Quantum Cohomology and Mirror Symmetry in Toric Varieties*, Nucl. Phys. **B440** (1995) 279–354, hep-th/9412236.

[26] M. Van den Bergh, *Non-Commutative Crepant Resolutions*, in "The Legacy of Niels Henrik Abel: The Abel Bicentennial, Oslo 2002", pages 749–770, Springer, 2004, arXiv:math/0211064.

[27] P. S. Aspinwall and D. R. Morrison, *Quivers from Matrix Factorizations*, Commun. Math. Phys. **313** (2012) 607–633, arXiv:1005.1042.

[28] A. Avram, M. Kreuzer, M. Mandelberg, and H. Skarke, *The Web of Calabi-Yau Hypersurfaces in Toric Varieties*, Nucl.Phys. **B505** (1997) 625–640, arXiv:hep-th/9703003.